J. Mol. Biol. **(1992) 223. 1121-1138**

Molecular Dynamics Simulations of Helix Denaturation

Valerie Daggett and Michael Levitt

Department of Cell Biology
Beckman Laboratories for Structural Biology
Stanford University School of Medicine, Stanford, CA 94305-5400, U.S.A.

(Received 29 July 1991; accepted 5 November 1991)

An understanding of the structural transitions that an a-helix undergoes will help to elucidate such motions in proteins and their role in protein folding. We present the results of molecular dynamics simulations to investigate these transitions in a short polyalanine peptide (13 residues) both *in vacuo* and in the presence of solvent. The denaturation of this peptide was monitored as a function of temperature (ranging from 5 to 200 °C). *In vacuo*, the helical state predominated at all temperatures? whereas in solution the helix melted with increasing temperature. The peptide was predominantly helical at low temperature in solution, while at intermediate temperatures the peptide spent the bulk of the time fluctuating between different conformations with intermediate amounts of helix, e.g. not completely helical nor entirely non-helical. Many of these conformations consisted of short helical segments with intervening non-helical residues. At high temperature the peptide unfolded and adopted various collapsed unstructured states. The intrahelical hydrogen bonds that break at high temperature were not fully compensated by hydrogen bonds with water molecules in the partially unfolded forms of the peptide. Increases in temperature disrupted both the helical structure and the peptide-water interactions. Water played a major but indirect role in facilitating unfolding, as opposed to specifically competing for the intrapeptide hydrogen bonds. The implications of our results to protein folding are discussed.

Keywords: helix-coil transitions; molecular dvnamics; protein folding; helix solvation; secondary structure fluctuations

1. Introduction

Motion and structural transitions are clearlv important for the biological activity of proteins and, as the most abundant form of secondary structure found in globular proteins. the dvnamics of the a-helix are particularly important. The motion and structural transitions that peptides undergo are also of interest to a variety of other processes including hormone-receptor interactions (Frv et *al.*, 1989), the efficacy of peptide drugs, vaccine development, immune function (Tainer et *al.*, 1984; Fieser et *al.*, 1987), membrane fusion (Takahashi, 1990), and possibly membrane transport activity (Vogel et *al.*, 1988). The inherent, stability of the α-helix is also of interest because of its probable role in protein folding.

One of the currently favored models for protein folding, the framework model! postulates that secondary structure is formed early in folding and that these preformed, marginallv stable fragments coalesce to form tertiary structure (Ptitsyn & Rashin, 1975; Kim & Baldwin, 1982). This hypothesis implies that secondary structure should be present under conditions where folding occurs spontaneously. Until recently most studies aimed at detecting secondarv structure within small peptides in aqueous solution were unsuccessful. There have now been numerous reports of helix formation in water at low temperature (usually 0 to 5 °C; Bierzynski et *al.*, 1982; Bradley et *al.*, 1990; Brown & Klee, 1977; Fry et *al.*, 1989; Goodman & Kim, 1989; Lyu *et al.*, 1990; Marqusee & Baldwin, 1987; Marqusee *et al.*, 1989; Shoemaker *et al.*, 1985, 1987). Even in the case of the most stable of these peptides, the helix content is low near physiological temperature. This suggests that other' pieces of secondary structure, or the protein scaffolding itself, are important during protein folding for stability of the nascent structure. Even so, a detailed understanding of helix dynamics aids in interpreting the motions and structural transitions of proteins.

It is unlikely that the unfolding and refolding of even a system as simple as an or-helix will ever be

0022-2836/92/041121-18 $03.00/0

characterized at the molecular level using experimental means. This is where simulations using detailed interatomic force fields are very important in increasing our knowledge of these processes, as they provide a complete and detailed description of atomic motion. For these reasons, we performed molecular dynamics simulations of polyalanine (13 residues) starting from the α-helix conformation, both *in vacuo* and in water at six different temperatures ranging from 5 to 200°C. Polyalanine was chosen for this study because it is "the simplest peptide that is able to adopt the α-helix conformation and because the helix-coil transitions and dynamics of polyalanine in *vacuo* have already been analyzed in detail (Daggett *et* al., 1991) and serve as a point of departure for these solution simulations. The present simulations were performed to address specifically how an α-helix unfolds, the effect of water on unfolding and the role of increasing temperature on these processes.

2. Methods

A 13-residue peptide of alanine was generated with close to ideal ϕ and ψ angles ($-60°$, $-40°$, respectively). The termini of the peptide were blocked (acetylated at the N terminus and amidated at the C terminus;. The potential energy function and associated parameters have been described (Levitt, 1983). Energy minimization and molecular dynamics were performed using the program ENCAD (Levitt, 1990) on a Silicon Graphics Iris 4D/240GTX computer. Water molecules were added around the peptide to fill a rectangular box, with walls at least 8 Å (1 Å = 0·1 nm) from any peptide atom, resulting in the addition of 735 molecules. The density of the solvent was set to the experimental value for the temperature of interest (0·999 g/ml at 278 K, 0·997 at 298, 0·988 at 323 K, 0·958 at 373, 0·916 at 423, and 0·861 at 473 K: Kell, 1967) by adjusting the volume of the box. We did not use a macroscopic dielectric constant for the simulations. This is equivalent to setting $\varepsilon = 1$ and it is assumed that the representation of the microscopic environment will approximate the desired dielectric effect when solvent molecules are present. Each of the resulting systems at different densities was then prepared for molecular dynamics. A total of 2000 cycles of conjugate gradient minimization was performed on the water molecules, followed by 2000 steps of molecular dynamics of the water molecules at the appropriate temperature to be used for the full simulation. The water molecules were then minimized again for 2000 cycles. Following preparation of the water molecules, the peptide atoms only were minimized for 2000 cycles, which was followed by minimization of the entire system (2000 cycles).

Following preparation of each system (corresponding to different temperatures), molecular dynamics was performed for 10^5 steps, or 200 ps. The system was brought to the target temperature by small momentum impulses for typically between 800 and 1000 steps, or less than 2 ps (Levitt, 1983). After this point, the temperature remained constant and no further scaling of the velocities was necessary. Periodic boundary conditions were used and the box volume was held constant during the simulation. The water model and methods for truncating the long-range interactions have been described by Levitt (1989) and a more extensive description is in preparation. In short, the water model is fully flexible with atom-centered charges. Structures were saved every 0·2 ps for analysis, yielding 1000 structures at each temperature. The preparatory steps and 200 ps of molecular dynamics took approximately 60 h of central processing unit time to perform.

In vacuo simulations were also performed at the 6 temperatures listed above to assess the importance of water to the dynamics of the peptide. The molecular dynamics protocol described above was employed.

Two other solution simulations were performed, beginning with the peptide in a β-strand conformation ($\phi = -120°$ and $\psi = 150°$). The solvated system contained 897 water molecules. The simulations were performed as described above at temperatures of 278 and 473 K for 100 ps.

3. Results

Molecular dynamics simulations of α-helical Ala13 were performed for 200 picoseconds at six different temperatures both with and without solvent. The overall properties of the dynamics of the peptide in solution as a function of the temperature are described. Next, the structural properties of the peptide and transitions it undergoes as a function of temperature and environment are presented. Finally, the peptide-water interactions are described.

(a) *Overall dynamic properties of the peptide in water*

Table 1 contains some of the overall properties of the peptide in solvent as a function of temperature. The accessible surface area decreased slightly with increasing temperature to 373 K, at 423 K the structure was slightly more exposed than the ideal α-helical starting structure, and at 473 K there was a large increase in the accessible surface area. The changes below 423 K are probably not significant. The rootmean-square (r.m.s.†) displacement of the

Table 1

Overall properties of polyalanine in water averaged over the entire simulation as a function of temperature

Temperature (K)	ΔA (Å^2)†	C$^\alpha$ r.m.s.d. (Å)‡
278	-28	1·3
298	-34	2·1
323	-29	2·1
373	-11	2.6
423	9	3·2
473	173	5·1

† The average change in solvent accessible surface area during the simulation. $\Delta A = (A(t) - A(t = 0 \text{ ps}))$ (Lee & Richards, 1971). All of the changes are relative to the accessible surface area of the helix at 278 K before molecular dynamics, 1129·6 Å^2.

‡ The average root-mean-square displacement (r.m.s.d.) of the α-carbon atoms from the starting structure between 100 and 200 ps. To eliminate Brownian motion, the r.m.s.d. is calculated after optimum superposition of the protein co-ordinates (Kabsch, 1976).

† Abbreviations used: r.m.s., root-mean-square; h, helix; c, coil; ts, transition state.

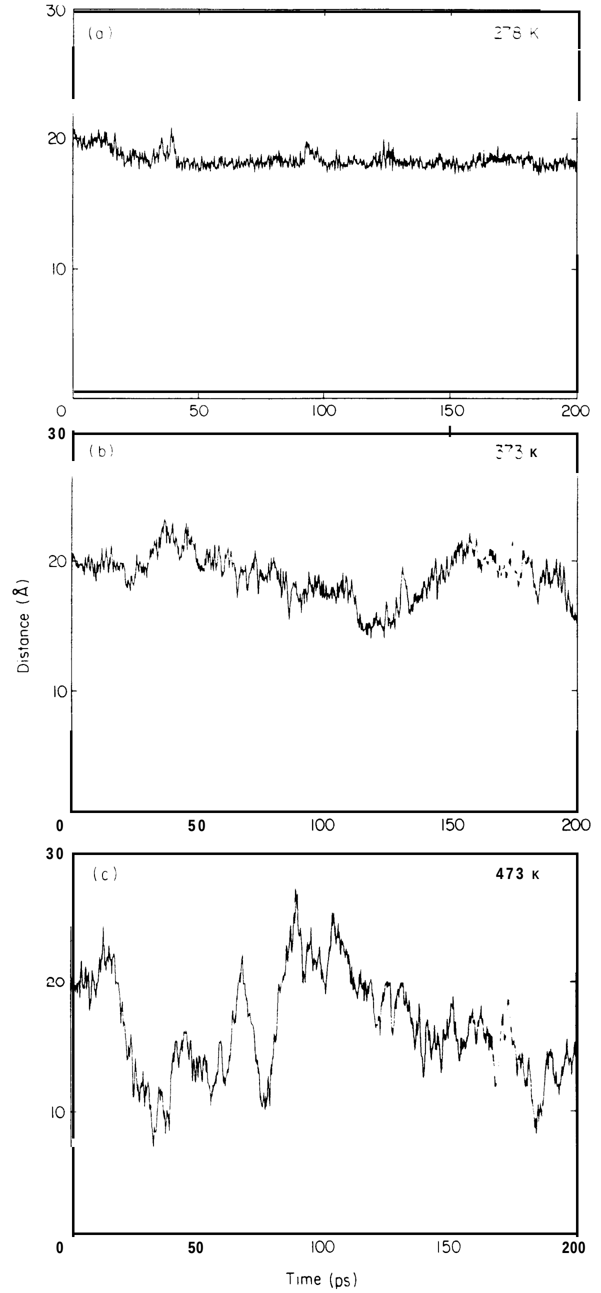

Figure 1. End-to-end distance for solution simulations at different temperatures as a function of time. The distances are between N of residue **1** and the carbonyl oxygen atom of residue 13.

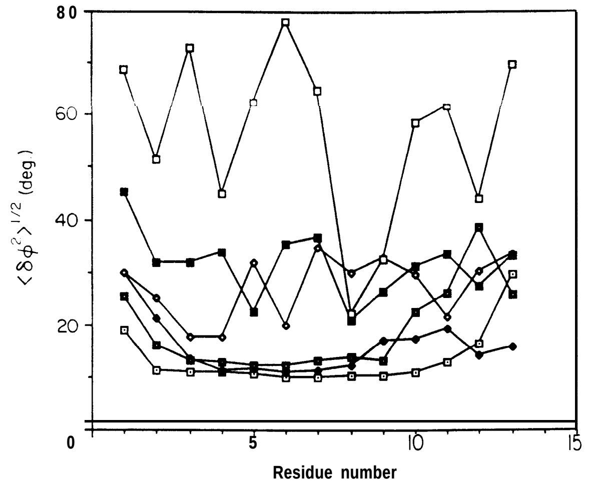

Figure 2. The root-mean-square fluctuations in the dihedral angle ϕ as a function of residue number and temperature. The following symbols distinguish the different simulations: (−⊡−) 278 K, (−◆−) 298 K, *(4)* 323 K, (−◇−) 373 K, *(4)* 423 K, and (−□−) **473** K.

or-carbon atoms from the starting structure increased with temperature (except at 323 K). These r.m.s. displacements were large, especially at 473 K, given the size of the peptide.

Figure 1 shows how the end-to-end distance of the peptide (computed from the amide nitrogen atom of residue 1 to the carbonyl oxygen atom of residue 13) varied with time. This distance serves as a measure of the overall motion of the peptide. The end-to-end distance of an ideal a-helix of this length would be -20 Å, while a completely extended conformation would be -45 Å. At 278 K the peptide became slightly more compact with time and then oscillated about the mean (r.m.s. fluctuation = 0·6 Å). The end-to-end distance was the same at 298 K and well maintained, but there were larger excursions from the mean compared to the lower temperature simulation (r.m.s. fluctuation = 0·9 Å). The deviation from the mean became even greater with increasing temperature (1·3, 1·6 and 1·9 Å at 323. 373 and 423 K, respectively). The structure became more compact, at 473 K and exhibited very large deviations from the mean (3·9 Å) as opposed to oscillating about the mean as observed at lower temperatures. All of the large distortions were toward more compact structures, except at 473 K. which did not contain helical structure (data presented below).

The fluctuations in the backbone dihedral angles also reflect the motion of the peptide. Figure 2 shows the angular variance in ϕ for each residue (similar behavior is demonstrated in ψ). The simulations at low temperature. 278 and 298 K, exhibited larger fluctuations at the ends of the structure than in the center. which is indicative of fraying of the helix. Fraying was also observed at 323 K, in addition to m&e extensive unfolding of the C terminus. Above 373 K, large fluctuations were observed throughout the peptide. At 473 K the fluctuations of some of the residues approached those expected for a completely random chain (~ 104”). However, the fluctuations remained low for residues 8 and 9.

(b) *Structural properties of the peptide both in* vacuo *and in solution*

To investigate how the helix content changed with time and temperature, we calculated the percentage of peptide residues that were helical. Following the approach of Daggett *et al.* (1991), a helical segment occurs when the ϕ and ψ values of

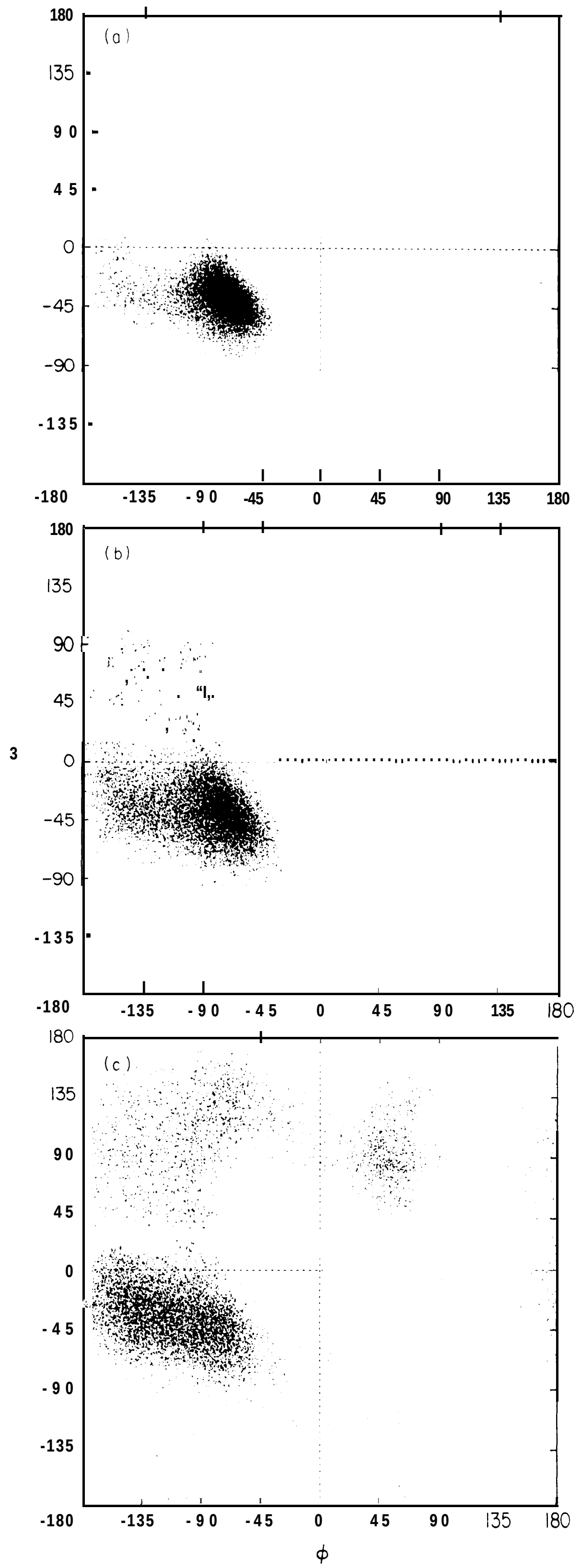

Figure 3. Ramachandran plots showing all dihedral pairs during the simulations at: (a) 278 K: (b) 423 K and (c) 473 K. Helical (ϕ, ψ) values are defined as those in the range $-100° \leq \phi \leq -30°$ and $-80° \leq \psi \leq -5°$.

at least three consecutive residues are within the helical region of conformational space. Using this definition a peptide of 13 residues can contain up to three helical segments. The range of allowed values was determined by investigating where ϕ and ψ cluster at low temperature when the peptide is predominantly helical (Fig. 3(a)). From the distribution of the Ramachandran plot we decided to use the following angular criterion of helicity: $-100° \leq \phi \leq -30°$ and $-80° \leq \psi \leq -5°$. Originally, we assigned helical values to those residues with (ϕ, ψ) angles within 30° of ideal a-helical angles ($-57°$, $-47°$, respectively). The cutoff was changed because the midpoint of the heavy cluster of values in Figure 3(a) is approximately ($-65°$, $-42°$) so that part of the cluster was considered non-helical according to the previous definition, although it is clearly an extension of the helical region.

Nearly all of the simulations showed drops in helix content with time (see Fig. 4). The peptide had similar average helix contents at 278, 298 and 323 K. although structural fluctuations were more prevalent at 298 and 323 K. At these temperatures, the peptide unfolds and refolds at the local level, while maintaining high degrees of helix content. The loss of local helical structure was fast: on average a residue left the helical state every four to five picoseconds and returned in less than one picosecond. Successive loss of local structure was observed for the higher temperature simulations and led to more global unfolding involving the entire sequence (as denoted by the low helix contents). The time scale of the global unfolding was temperature dependent, spanning 25 to 200 picoseconds. The peptide quickly unfolded at 473 K and did not regain helix content with time. The peptide did form appreciable amounts of p-structure. however, at this temperature (Fig. 5). During approximately 10 % of the simulation, a β-turn existed between residues 5 and 9. which may partly explain the low dihedral fluctuations shown in Figure 2. Overall, the excursions from the helical state involved everything from slight deviations from the a-helical conformation, local short-lived turn formation, to complete disruption of the structure. (Fig. 6 shows some representative structures at. 473 K.)

Figure 7 shows melting curves for the simulations performed both *in vacuo* and in solution. Helix content, was evaluated in three ways: (1) helical residues were identified by the individual dihedral angles (ϕ, ψ); (2) helical segments were defined as having at least three consecutive residues with helical (ϕ, ψ) angles; and (3) the helix content was computed as the average number of intact native $i \rightarrow i + 4$ hydrogen bonds expected for an a-helix + 4 residues. The first definition measures local helix content while the others reflect more global structure. In the solution simulations, the different definitions yielded similar curves (Fig. 7). Increases in temperature clearly led to substantial decreases in helix content, in solution. In contrast, in the absence of water the peptide exhibited high helix

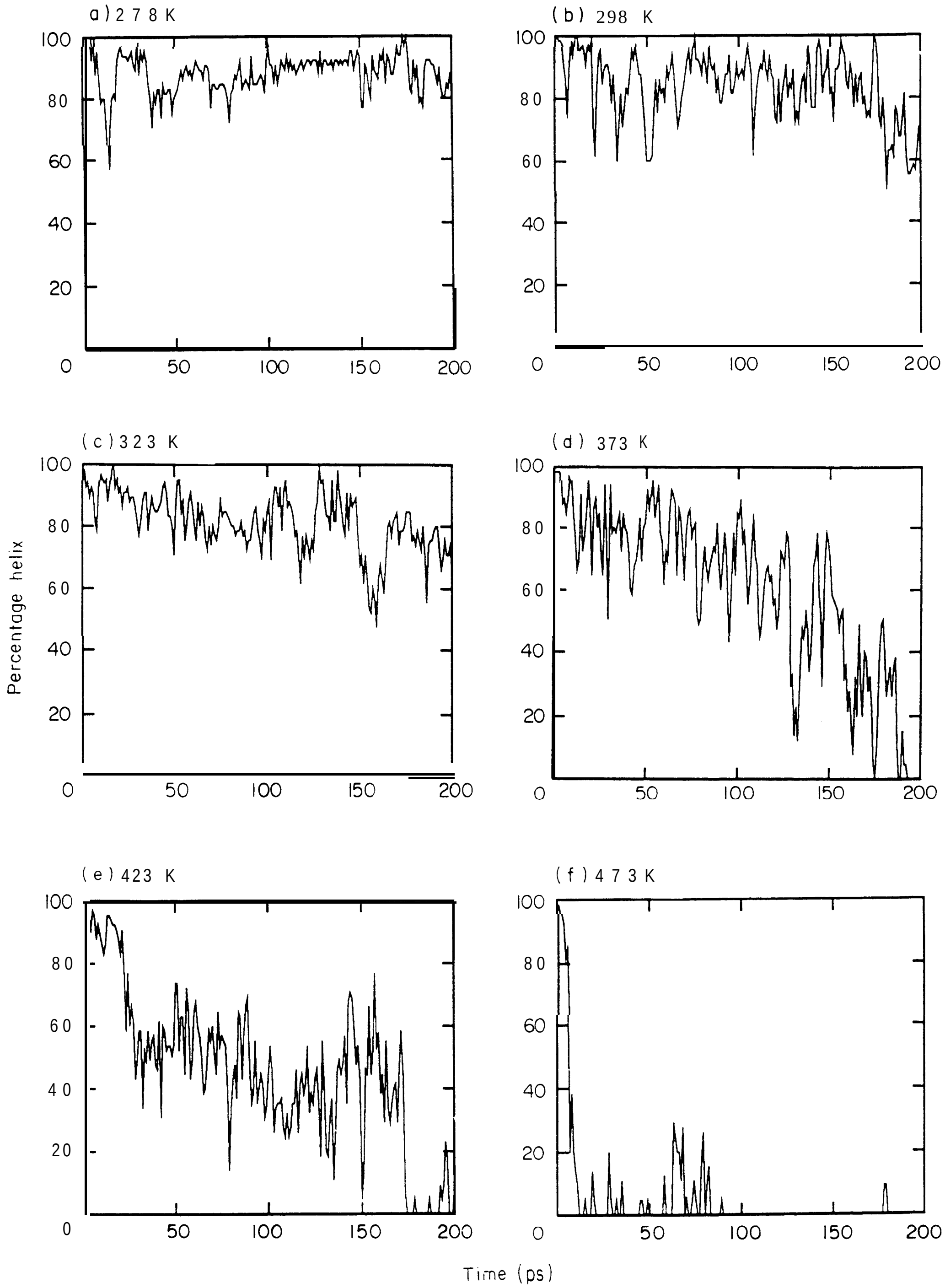

Figure 4. (a) to (f) Percentage of helix at different temperatures (averaged over 1 ps intervals) as a function of time. The method of identifying helical segments ($\geq$ helical 3 residues) based on (ϕ. ψ) values was used.

contents even with increasing temperature. It should be emphasized that only the trends in helix content. either with time or temperature. are meaningful. The absolute helix contents cannot be compared directly to experimental values because the definition is somewhat arbitrary. although outside the bounds of dynamic fluctuations within well-maintained portions of secondary structure (< 15").

The degree of conformational sampling at different temperatures can be seen in Ramachandran plots, showing all (ϕ, ψ) values explored during the simulations. At low temperature, the peptide was predominantly helical, with most points clustering in the lower left quadrant of the plot (Fig. 3(a)). At higher temperature the peptide began to explore more of the B-region of conformational space (Fig. 3(b)). At **473** K the

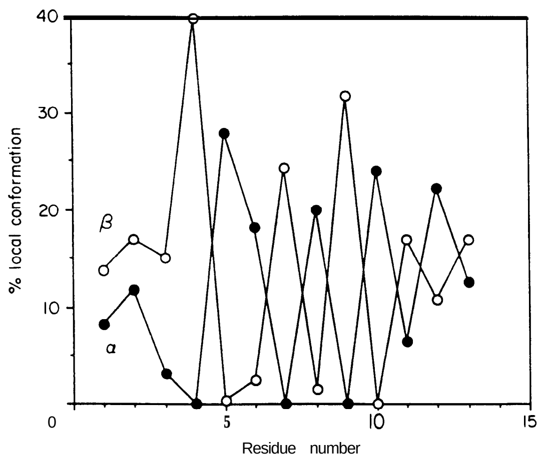

Figure 5. Percentage of local structure at 473 K as a function of residue number from 0 to 100 ps. The filled circles represent a-helix and the open circles are for p-structure. The structure assignment' was based on dihedral angle pairs (or-helix. $-100° \leq \phi \leq -30°$. $-80° \leq \psi \leq -5°$ and p-structure $-169° \leq \phi \leq -89°$. 83" $\leq \psi \leq 165°$).

peptide explored most of (ϕ, ψ) space (Fig. 3(c)). In addition to showing the amount of conformational space sampled as a function of temperature, these plots demonstrate that our definition of helix content is reasonable. For example, the definition would be inappropriate or misleading if all of the (ϕ, ψ) values clustered around the a-helical region such that a small change in the angular cutoff would lead to a large change in the calculated helix content. From the helical region the (ϕ, ψ) values drifted toward higher ψ and lower ϕ values until finally the P-region was reached. Manv of the structures falling along the diagonal near the helical region are distorted helices, with carbonyl groups tilting out to interact with the solvent.

Other helical properties can also be determined using the definition described above for identifying helical segments (Table 2). In solution. the average helix length decreased with increasing temperature. Multiple helices were present. although not dominant in solution. while a single long helix was the norm *in vacuo*.

As would be expected. intramolecular hvdrogen bonds were important in stabilizing the' helical conformation. The $i \rightarrow i + 4$ hydrogen bonds typical of an ideal a-helix were the most populated hydrogen bonds at low temperature (Table 3). With increasing temperature other hydrogen bonds became populated (e.g. $i \rightarrow i+5$) (compare $i \rightarrow i+4$ hydrogen bonds to all observed main-chain hvdrogen bonds; Table 3), although the total number of main-chain hvdrogen bonds decreased with increasing temperature. At 278 K, the number of hydrogen bonds was essentially constant with time. Many of the non $i \rightarrow i+4$ hydrogen bonds involved the blocking groups. which are not counted even if they do adopt an $i+4$ spacing. Above 373 K, the $i \rightarrow i + 4$ hydrogen bonds became less populated than the other main-chain hydrogen bonds after approximately 70 picoseconds of molecular dynamics. which correlates roughly with unfolding of the helix (Fig. 4). At 473 K. however, the number of $i + 4$ hvdrogen bonds dropped almost immediatelv. All of the hydrogen bond trends observed correlated with the changes in helix content with either time or temperature (data not presented), namely, when the intrahelical hydrogen bonds broke the helix content decreased.

(c) Structural transitions

Although the simulations were too short to reach equilibrium, fast events can be treated as if at equilibrium. An example of these fast events is the single residue helix $\rightarrow$ coil (h $\rightarrow$ c) transition. The changes in free energy for this process were determined both *in vacuo* and in solution. Residues within helical regions were defined as described above. The free energy was computed from the average waiting time (τ) for the h$\rightarrow$c and c$\rightarrow$ h transition for each residue; these waiting times reflect the relative populations of the different conformations. The ratio of the waiting times was then averaged over all residues during the **100** to

Table 2

Helical properties averaged over the 100 to 200 ps interval of the simulations as a function of temperature and environment

Temperature (K)	(Helix length) (residues)		So. helices/structure		% of time with > 1 helix	
	Solution	Vacuum	Solution	Vacuum	Solution	Vacuum
278	11·4	12·3	1·0	1·0	2	0
298	843	11·7	1·2	1·0	18	l
323	9·4	12·0	1·1	1-o	7	l
373	5·6	11·2	1·0	1·0	16	3
423	4·7	10·9	0·8	1-o	14	4
473	3·0	10·5	0·0	1·0	0	4

The method of defining helical segments was used to determine the helical properties (e.g. (ϕ, ψ) of at least 3 consecutive residues are required to be within the helical region of conformational space as described in the text). The following properties are given: the average helix length, the average number of helical segments per structure. and the percentage of the simulation time that more than 1 helical segment was present.

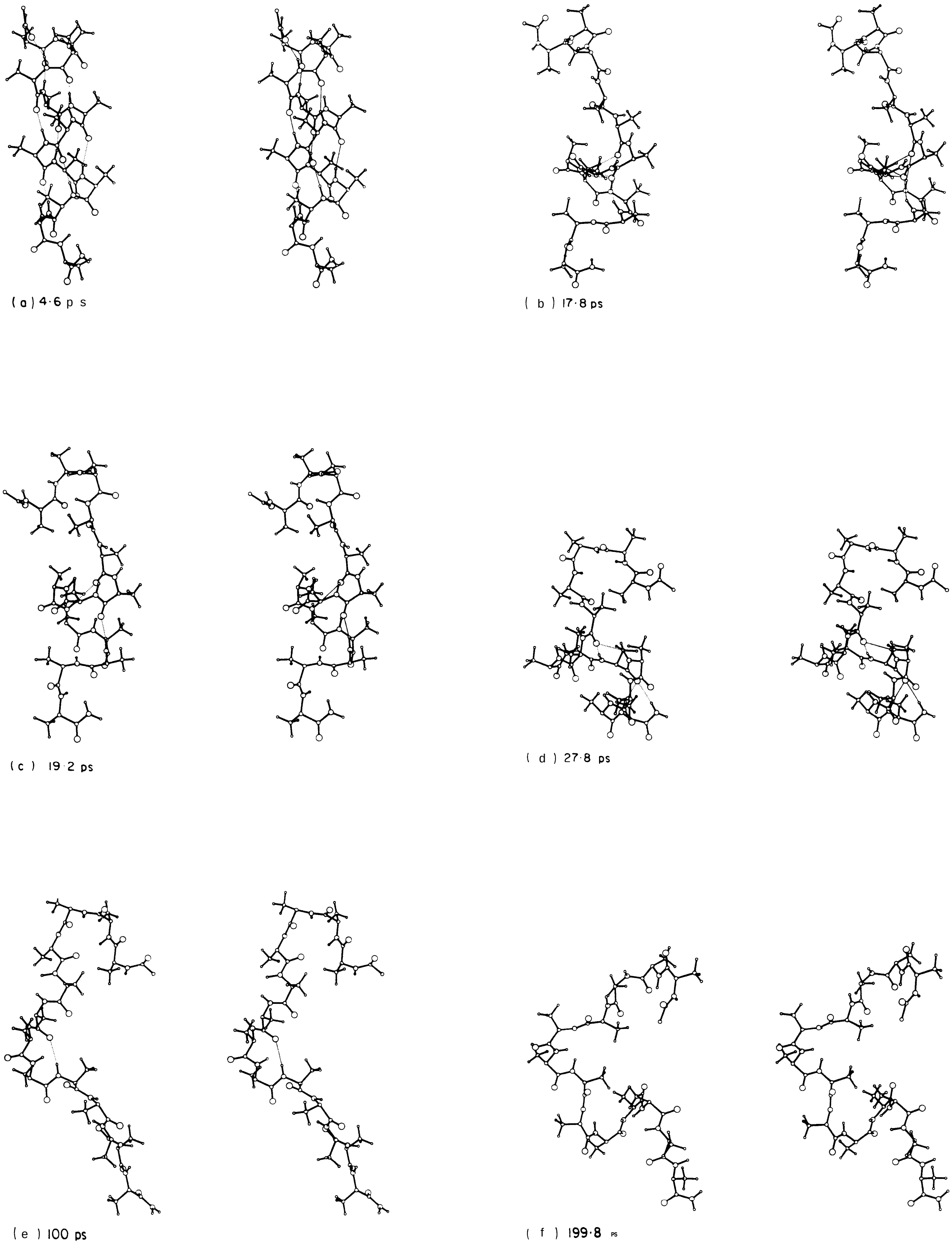

Figure 6. (a) to (f) Stereoviews of snapshots from the high temperature solution simulation at 473 K: (a) 4·6 ps with 85% helix: (b) 17·8 ps with 0% helix; (c) 19·2 ps, 23% helix; (d) 27·8 ps. 46% helix: (e) 100 ps. 0% helix: and (f) 199·8 ps. 0% helix. Intrapeptide hydrogen bonds are shown as broken lines.

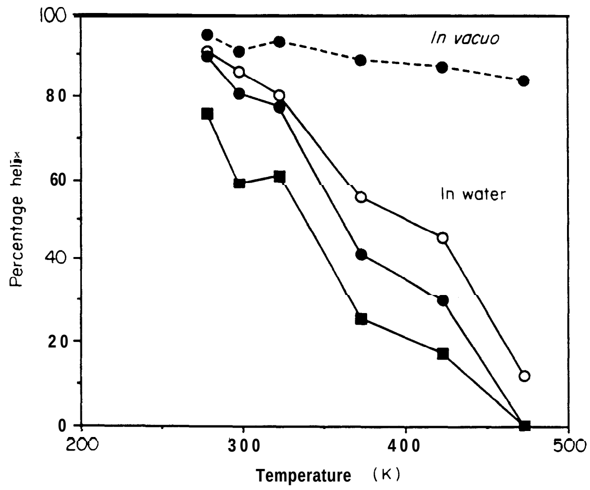

Figure 7. Average percentage of helix (averaged over the 100 to 200 ps time interval) as a function of temperature. The 2 curves marked by filled circles used the helix definition that requires repeating structure: the broken line represents the simulations in *vacuo* and the continuous line the situation in solution. The line with the open circle is for the solution simulation using the helix definition that measures only local structure and the final curve (filled squares) used the hydrogen bond definition of helix content.

200 picosecond interval of the simulation ($K_{c\rightarrow h} = \tau_{h\rightarrow c}/\tau_{c\rightarrow h} = k_{c\rightarrow h}/k_{h\rightarrow c}$, $\Delta G_{c\rightarrow h} = -RT \ln K_{c\rightarrow h}$; Table 4). This approach of using waiting times for calculating equilibrium constants is equivalent to using the ratio of the populations, e.g. $K_{c\rightarrow h}$ = [% helix]/[% coil]. Determination of the waiting times enables us to extract additional information about the frequency and rates of these transitions. The waiting times multiplied by the observed number of transitions will not necessarily account for the full 100 ps analysis time because transitions were counted for h→c→ h, such that towards the end of the time interval the helical state may not have been regained. For the 473 K water simulation, the free energy change is reported for 0 to 100 picoseconds of the simulation because the number of structural transitions was very low during the second half of the simulation.

The free energy change for the $h\rightarrow c$ transition decreased with increasing temperature in solution (Fig. 8). Transitions to non-helical conformations were unfavorable below 423 K, although the free energy change was still near ET. In *vacuo*, such transitions were unfavorable at all the temperatures studied and the free energy change is independent of temperature. Comparison of the two curves shows clearly that the h→c transition was more favorable in water than in *vacuo*. From these curves, the enthalpy and entropy changes for the helix to coil transition can also be estimated (using the familiar relationship, AG = AH- TAS and plotting AG *versus T*). In water, the conversion of a residue from the helical to the non-helical region of conformational space was driven by an entropy change of 9·0 cal/mol per K per residue and opposed by an enthalpy change of 3·7 kcal/(mol-residue). *In vacuo*, AH = 0·72 kcal/(mol-residue) and **AS = – 2·0** cal/mol per K per residue, which indicates that there was little entropic and enthalpic distinction between the helical and non-helical states. The main reason

Table 3

Inter- and intramolecular hydrogen bonds and water contacts as a function of temperature and starting conformation

	Temperature (K)							
	a-Helix						Extended P-strand	
Property†	278	298	323	373	423	473	278	473
No. C=O... HN HB	9·2	8·9	9·0	7·5	7·2	2.6	0·2	0·8
No. $i\rightarrow i+4$ C=O... HN HB	6·1	5·0	5·4	3·8	3·0	0·6	0·0	0·0
No. $i\rightarrow i+5$ C=O... HN HB	0·0	0·9	0·3	0·9	1.2	0·4	0·0	0·0
Average **accessible** surface area (Å^2)	1102	1096	1101	1119	1139	1303	1529	1468
No. water molecules contacting peptide	54·1	51.6	52.8	48·8	43.2	45·8	85·0	60·1
No. HN... H_2O HB	2.3	2·1	1·6	1·9	1·5	3·8	10.8	6.2
No. HN... H_2O contacts	2.8	3·0	3·0	4·2	3·9	8·4	13.3	10.8
No. C=O... H_2O HB	12·0	11.3	9·5	8·5	7·3	8·2	20.0	11·8
No. C=O... H_2O contacts	19.4	19.3	19·6	19.9	19.1	23.3	34.6	30.6
No. H_2O... H_2O HB	1202	1187	1161	1116	1064	999		

HB, hydrogen bonds. **Contacts** were defined as having interatomic distances ≤2·6 Å, while hydrogen bonds had the added requirements that the **donor-H..** .acceptor angle was within 45° of linearity.

† All properties considered were averaged over the full duration of the simulations (200 ps for the helical simulations and 100 ps for the β runs).

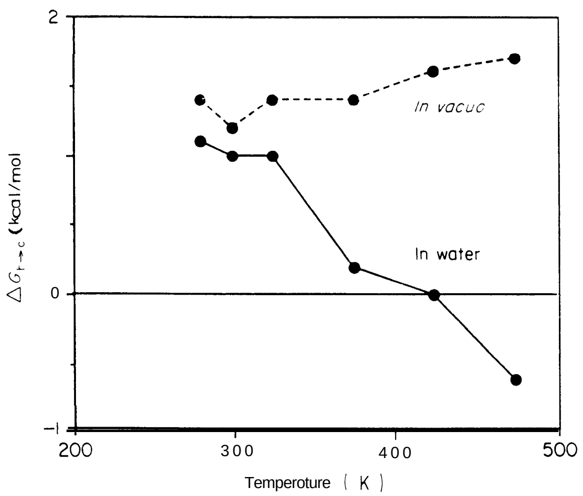

Figure 8. The free energy change for the single residue helix to coil transition both *in vacuo* and in solution as a function of temperature. The free energy changes were calculated as described in the text for the 100 to 200 ps interval of the simulation, except at 473 where the average was done between 0 and 100 ps.

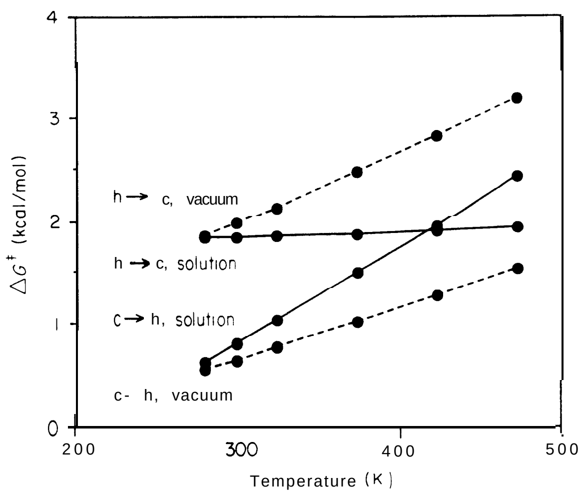

Figure 9. The temperature dependence of the free energy of activation for the single residue h → c and c → h transitions. Calculation of $\Delta G^{\ddagger}$ is described in the text.

for the lack of distinction between the two states *in vacuo* was that when a residue left the helical state *in vacuo* it never strayed far from the helical region of (ϕ, ψ) space.

The rates for these h ↔ c transitions were also investigated as a function of the environment. Rate constants for the single residue transitions were approximated as the inverse of the waiting times. From the rate constants, Arrhenius plots were constructed to obtain activation energies ($\ln k$ *versus* $1/T$, where the slope $= E_a/R$, not shown). The activation energy in solution was 2·42 kcal/mol for the h → c transition, and − 1·25 kcal/mol for c → h. The corresponding activation energies *in vacuo* were 0·68 and − 0·09 kcal/mol for the h → c and c → h transitions, respectively. The entropy of activation was determined from the y-intercept of the Arrhenius plots (the intercept $= \ln A$, $\Delta S^{\ddagger} = R \ln (Ah/ek_B T)$, where h is Planck's constant and k_B is the Boltzmann constant). From the activation energies and entropies, the enthalpy and free energy of activation were determined for both transitions at each temperature ($\Delta H^{\ddagger} = E_a - RT$ and $\Delta G^{\ddagger} = \Delta H^{\ddagger} - T\Delta S^{\ddagger}$). Both the activation enthalpy and entropy changes varied with temperature: the activation enthalpy decreased by 0·4 kcal/mol in 200° and $\Delta S^{\ddagger}$ decreased by 1·1 cal/(mol-degree). The free energies of activation changed most dramatically.

Figure 9 shows the temperature dependence of the activation free energies for the single residue transitions, both *in vacuo* and in solution. In all cases, except for the h → c transition in solution, the free energy of activation increased with increasing temperature, reflecting the increased difficulty of finding the relatively ordered transition state structure from progressively more disordered states (Fig. 3). Comparison of the solution and vacuum curves for the h → c (or h → ts, rather, where ts is the transition state structure en route to the non-helical state) indicate that the process was more favorable in solution. In *vacuo*, the c → ts transition exhibits the same temperature dependence as h → ts. The c → h transition in solution shows a much steeper increase in the activation energy with temperature. As non-helical states further from the helical region of conformational space are adopted with increasing temperature (Fig. 3), it becomes increasingly difficult to form the transition state structure and this effect is most dramatic in solution because of the ability of the solvent to aid in stabilization of the non-helical state.

From the free energy differences between the states and the activation free energy changes, free energy profiles were constructed. Unfortunately, only the free energy difference between the helix, coil and the transition state structure between them can be determined, and not the absolute free energies of these states. Therefore, we do not have a point of reference for placement of the profile along the y-axis. In principle, changes in the relative positions of any of the three states can be altered when the free energy changes with temperature. The three simplest possibilities are: (1) the free energy of the helical state, G_h, is independent of temperature; (2) the free energy of the transition state, G_{ts}, is independent of temperature; and (3) the coil state, G_c, is independent of temperature. The first two cases are most likely. Since the non-helical state is heterogeneous, more and different states will be available with increasing temperature (Fig. 3), making changes in G_c likely. Since the transition from a helical to a non-helical conformation involves simple dihedral rotations it is reasonable to assume that the absolute free energy of the transition state is essentially independent of temperature. Considering the wide range of helical (ϕ, ψ) values allowed, some differences in G_h would be expected. Therefore, G_{ts} being independent of temperature is

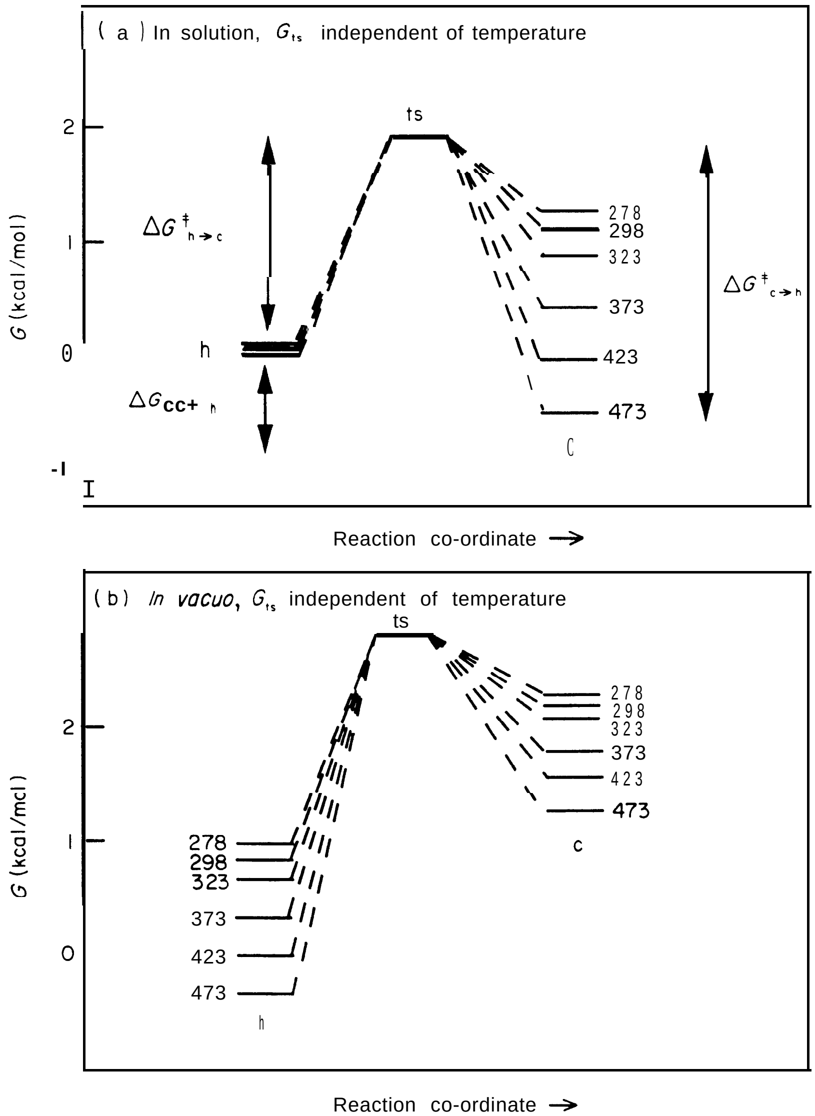

Figure 10. Free energy profiles for the single residue h → c transition as a function of temperature and environment: (a) in solution and (b) *in* vucuo. The transition state is denoted by ts. Determination of $\Delta G_{h \leftrightarrow c}$, $\Delta G^{\ddagger}_{h \to c}$ and $\Delta G^{\ddagger}_{c \to h}$ is described in the text. The absolute free energies of the h, c and ts states cannot be determined. So, we do not have a point of reference for positioning the profile along the y-axis. G_{ts} was assumed to be independent of temperature SO that positioning of the h and c states is relative to ts. The rationale for this choice is given in the text.

probably the most reasonable possibility and is used here, but the other alternatives cannot be ruled out,.

At low temperature in solution, the helical state was clearly favored, such that even when the non-helical state was attained, the free energv of activation to reach the transition state was low. making conversion back to the helical state facile (Fig. 10(a)). The free energy of activation for the c → h transformation changed dramatically with temperature, unlike the h → c transition. At high temperature it became more difficult to traverse the barrier to get back to the helical state. The free energy of the helical state was essentially independent of temperature in solution. In *vacuo*. however, the free energy difference between the helix and coil states was independent of temperature such that the free energies of both the helical and coil state dropped with increasing temperature, with G_h always less than G_c at a particular temperature (Fig. 10(b)). That the free energy of the helical state would decrease in this case with temperature can be rationalized because the peptide is able to adopt more conformations at high temperature that are still considered to be helical according to our definition, thereby increasing the entropy. In the case of the solution simulations, the water interactions seem to counteract this effect. Within this same context, the entropy for going from the helical conformation to the transition state becomes more unfavorable because of the necessity of both finding and "freezing" the transition state geometry. The entropy of activation for the c → ts conversion also became more unfavorable in both environments with increasing temperature, and, supporting the

Table 4
Helix-coil transitions as a function of temperature and environment during the 100 to 200 ps interval of the simulations

Property	Temperature (K) 278	298	323	373	423	473
A. $c \leftrightarrow$ in vacuo						
⟨No. tran./res.⟩	9	13	11	18	22	24
$\langle\tau_{h\to c}\rangle$ (ps)	5·3	4·4	4.6	3·3	3·4	3·2
$\langle\tau_{c\to h}\rangle$ (ps)	0·4	0·6	0·5	0·5	0·5	0·5
$K_{c\to h}$	12·2	7·3	9·5	6.7	6·9	5·9
$\Delta G_{c\to h}$ (kcal/mol)	−1·4	-1.2	−1·4	−1·4	-1.6	−1·7
B. $c \leftrightarrow h$ *in solution*						
⟨No. tran./res.⟩	12	26	20	38	39	35
$\langle\tau_{h\to c}\rangle$ (ps)	5·0	3·0	3·6	1·4	1·1	0·8
$\langle\tau_{c\to h}\rangle$ (ps)	0·6	0·5	0·8	1·0	1·1	1·4
$K_{c\to h}$	8·0	5·9	4·5	1·4	1·0	0·5
$\Delta G_{c\to h}$ (kcal/mol)	−1·1	−1·0	−1·0	−0·2	0·0	0·6
C. $hc_ic \leftrightarrow hh_ic$ *in solution*						
⟨No. tran./res.⟩		3	3	5	9	4
$\langle\tau_{hhc\to hcc}\rangle$ (ps)		3.3	2·6	2·8	2·6	6·0
$\langle\tau_{hcc\to hhc}\rangle$ (ps)		7·0	5·0	5·6	3·5	3·0
$K_{hcc\to hhc}$		2·1	1·9	2·0	1·3	0·5
$\Delta G_{hcc\to hhc}$ (kcal/mol)		−0·4	-0.4	−0·5	−0·2	0·6
D. $cc_ic \leftrightarrow ch_ic$ *in solution*						
⟨No. tran./res.⟩		—		8	13	18
$\langle\tau_{chc\to ccc}\rangle$ (ps)				3·3	3·0	2·2
$\langle\tau_{ccc\to chc}\rangle$ (ps)				3·1	1·9	1·0
$K_{ccc\to chc}$	--			1.0	0·6	0·4
$\Delta G_{ccc\to chc}$ (kcal/mol)	--			0-0	0·4	0·8

Transitions are defined as occurring between residues within the helical region of conformational space, based on the (ϕ, ψ) values (see the text), and any other conformation. The first 2 processes represent single residue transitions. hcc↔hhc depicts helix propagation, and the final process is helix nucleation. At 473 K the transitions were evaluated from 0 to 100 ps because there were very few transitions during the 2nd half of the simulation. ⟨No. tran./res.⟩ is the average number of transitions observed during 100 ps. The waiting times. τ, were determined directly from the simulation. from which K and AG were determined (e.g. $K_{c\to h} = \tau_{h\to c}/\tau_{c\to h}$ and $\Delta G = -RT \ln K$). All of the entries were averaged over time and all residues. The values for the equilibrium constants may be slightly different than what is computed from the waiting times given: the difference is because the equilibrium constants were calculated considering more significant figures than are given in this Table.

notion of hindered rotation in adopting the transition state structure, the entropy of activation in solution for the c → ts transition was ten times more unfavorable than for h → ts.

The propensitv for helix propagation was also monitored for the solution simulations above 278 K ($hc_ic \rightarrow hh_ic$; Table 4); at 278 K there were too few transitions to obtain good statistics. Even at higher temperatures there were very few transitions (3 to 9) and we are probably at the limits of analyzing these transitions as fast events. As for the single residue transitions? the free energy change for the process in solution was temperature dependent, with the tendency for conversion of a non-helical residue to the helical state becoming less favorable with increasing temperature. Below 373 K it was harder to convert a residue to a helical conformation at the helix-coil interface than the background level for the single residue transition. At 373 and *423* K, propagation of the helix was slightly more favorable than the single residue transitions. Thus, at these temperatures the neighboring helical residue facilitated conversion. The equilibrium constants for helix propagation correspond to the s parameter of the Zimm-Bragg model (discussed further below). Furthermore, the changes in enthalpy and entropy for helix propagation were obtained from a plot of the free energy of propagation (given in Table *4) versus* temperature as described for the single residue transitions in Figure 8. The resulting values were $\Delta H_{propagation} = -2{\cdot}1$ kcal/(mol-residue) and $\Delta S_{propagation} = -5{\cdot}1$ cal/mol per K per residue. These values should be comparable to the enthalpy changes for the helix–coil transitions determined experimentally; however, thev can be viewed as only approximate because the free energv change with temperature was not strictly linear (correlation coefficient of 65%).

Finally, helix nucleation within a non-helical region was investigated above 373 K (Table 4, $cc_ic \rightarrow ch_ic$). At lower temperature this process occurred infrequently. The free energy change for the process was unfavorable. This transition was more difficult than both the single residue transitions and propagation. Therefore, the neighboring non-helical residues helped to maintain the central residue in a non-helical conformation. The intrinsic nucleation parameter, σ, can be determined from the equilibrium constants for nucleation and propagation $\langle K \rangle_{ccc \rightarrow chc} = \sigma\ s$. The nucleation parameter was independent of temperature below 473 K and equal to 0·4, at 473 K σ = 0·8. A macroscopic σ equivalent to the nucleation parameter from the Zimm-Bragg model was also calculated from equation 3b of their paper (Zimm & Bragg, 1959) using the helix contents and s parameters described above. The resulting values were 10^{-3} to 10^{-4}. The difference between this macroscopic σ and the intrinsic, microscopic value is due to the different definitions for the h and c transitions. The earlier Zimm-Bragg model defines helical segments by hydrogen bonds and therefore nucleation involves at least three residues adopting local helical structures to form the first hydrogen bond. We cannot evaluate this process? as there were too few occurrences. Nucleation for a five-residue segment is more difficult than one would predict from the intrinsic values (e.g. in the worst case where each transition occurred independently, the macroscopic value would be σ^3, or approximately 0·125). The process is evidently more complicated.

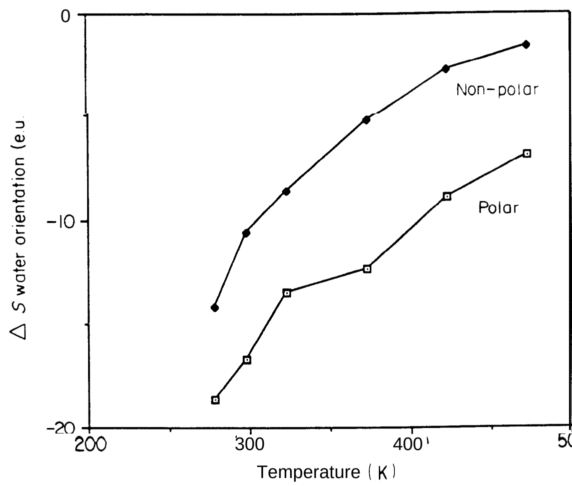

Figure 11. The orientational entropy of the water molecules near non-polar residues and near polar residues. This entropy is determined by comparing the distributions of water molecule positions and orientations to those expected for a randomly oriented solvent, using the equations $\Delta S = k_B \Sigma n_i \ln p_i$, where k_B is the Boltzmann constant, n_i is the observed number, and p_i is the ratio of n_i to the number expected for a uniform distribution (Levitt & Sharon, 1988).

(d) *Peptide-water interactions*

(i) *Water motion*

The water molecules in the simulation can be broken down into different classes for analysis: water molecules in contact with polar peptide atoms (<3·1 Å): water molecules in contact with non-polar peptide atoms (< 4·5 Å); water molecules not in these groups but within 10 Å of the peptide: and bulk water. The water molecules were extremely mobile during the simulation and exchange between the different groups readily. The diffusion of the molecules was essentially the same for the different classes at all temperatues, differing by no more than 0·06 Å^2/ps and generally less than 0·02 Å^2/ps. The diffusion increased with temperature, by an order of magnitude, between 278 and 473 K (0·13 and 1·80 Å^2/ps, respectively for bulk water). The mean residence time for the different shells also differed. The average time that any particular water molecule spent, in contact with the peptide, with either polar or non-polar groups, was extremely short and decreased from 0·7 picosecond at 273 K to 0·3 picosecond at 473 K. Although the water molecules exchanged quickly between the different shells throughout the simulation, the peptide did influence the nearby water molecules. The orientational entropy of the water molecules, compared to a completely disordered state: increased with increasing temperature (Fig. 11, calculation of the entropy has been described by Levitt & Sharon (1988)). The orientational effect of the non-polar and polar groups of the peptide changed by approximately the same degree with temperature. At high temperature, the non-polar groups had little ordering effect on the water molecules (i.e. ΔS close to zero), while the polar groups were still able to constrain the motion of the nearby water molecules.

(ii) *Water-peptide contacts*

The number of water molecules in contact with the peptide depends on the extent to which the conformation is open and exposed to solvent. It also depends on the properties of the water molecules themselves. Thus, at high temperature, the peptide unfolds, becoming less compact and more exposed to solvent (Table 3). Water properties also change at higher temperature: the density decreases? reducing the number of water molecules in contact with a given exposed group and the probability that a water molecule in contact with a given polar group will actually form a hydrogen bond also decreases. The average number of water molecules in the hydration shell immediately around the peptide decreased with increasing temperature (Table 3), except for the slight increase in the number of contacts from 423 to 473 K. These results indicate that specific hydration became patchy at high temperature (the average amount of surface area increased from 20·4 to 28·4 Å^2/water molecule). This decrease in hydration was a bit surprising given that the accessible surface area increased, exposing more polar main-chain atoms to water. That the number of water molecules containing the peptide does not increase throughout the temperature range and scale with the surface area is due to the decrease in water density at high temperature. The types of water contacts were then broken down further.

Table 3 also contains the average number of contacts between the amide hydrogen of the peptide with water molecules (d(HN . . . O_{water}) ≤ 2·6 Å) and specific hydrogen bonds (d(HN . . . O_{water}) ≤ 2·6 Å and θ(N–NH–O) within 45° of linearity) at each temperature. At low temperature (278 K) essentially all of the water molecules in contact with the amide peptide groups formed hydrogen bonds. At higher temperatures, the decrease in densitv and the additional entropy led to both a de&ease in contacts and hvdrogen bonds (Table 3). AT 473 K. where essentially all of the amide hydrogen atoms were exposed. both the number of hydrogen bonds and contacts were high. in spite of the low density and increased water motion. In the extended P-strand. both the number of hydrogen bonds and contacts were greater than in the simulation beginning from an a-helical conformation. The values decreased with increasing temperature, however, as the structure collapsed and exposure of the main chain decreased. The increase in entropy with increasing temperature also led to decreases in the number of water-water hydrogen bonds (Table 3).

Table 3 also contains the corresponding water contacts and hydrogen bonds to the carbonyl oxygen atoms of the peptide. where the distance cutoff is between the carbonyl oxygen atom and either. or both. hydrogen of a water molecule. At low temperature (278 and 298 K) there was a discrepancy between the average number of contacts and hydrogen bonds. but the trends with time were the same. It appears that there is some competition for the two hydrogen bonding sites on the carbonyl oxygen atom. since the percentage of the contact water molecules that form hydrogen bonds with the carbonyl oxygen atom is lower than with the amide hvdrogen atoms (82 % *versus* 62 % at 2 78 K . Table 3). At higher temperatures (323. 373. 423 K) the average number of hydrogen bonds decreased and the C=O . . . water contacts increased slightly. At 373 K the number of contacts increased dramatically near the end of the simulation where the helix content dropped below 20%. At 473 K all the carbongl groups were almost completely exposed to solvent throughout the simulation, the number of contacts was high but the number of actual C=o . . . water hydrogen bonds was at approximately the same level as at lower temperatures where the helix was intact. The number of contacts and helix content were negatively correlated, to varying degrees. demonstrating that the contacts increased as the helix content dropped (data not presented). Again the extended P-strand participated in both more contacts and hydrogen bonds with water than did the cc-helix. Comparison of the highest temperature a-helix and /?-strand simulations indicates that the unfolded form of the helix was not extended and instead more closely resembled the collapsed state

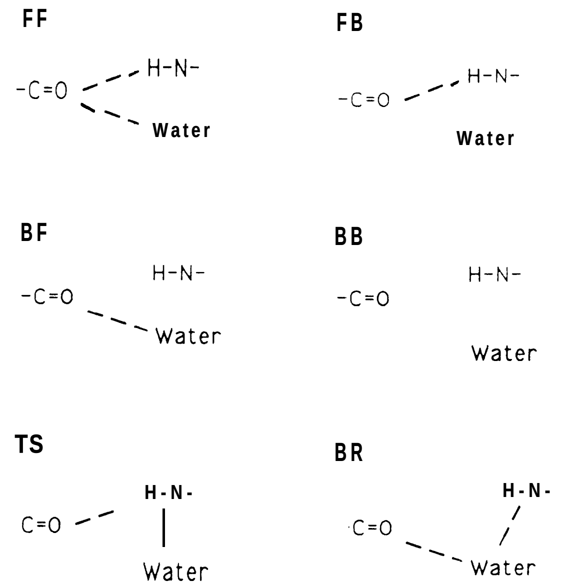

Figure 12. Nomenclature for the intra- and intermolecular hydrogen bonds with the carbonyl oxygen atoms of the peptide. Hydrogen bonds are defined as having distances between the carbonyl oxygen atom and the closest amide hydrogen or water hydrogen atom ≤ 2·6 Å. for the first 9 residues (the final 4 carbonyl oxygen atoms do not have peptide hydrogen bonding partners). The abbreviations used are: FF, both peptide and water hydrogen bonds are formed: FB. peptide hydrogen bond is formed while the hvdrogen bond to water is broken: BF. the peptide hydrogen bond is broken and the water hydrogen bond is formed: BB. both broken: TS. S-centered hvdrogen bond between water and the peptide: and BR.' water molecule bridging carbonyl and amide groups.

reached bv the P-strand at high temperature, at least by these criteria.

(iii) *Correlated hydrogen bonding*

At any time, a particular peptide carbonyl group can be hydrogen bonded to a peptide HN group, to a water molecule, to both, or to neither. In an attempt to elucidate the role of water in breaking the peptide hydrogen bonds, distances between the carbonyl oxygen atoms and the nearest amide hydrogen and water hydrogen atoms were computed as a measure of hydrogen bonding. Different hvdrogen bonding scenarios were considered: both the intrapeptide and peptide-water hvdrogen bonds were formed simultaneously (FF); the main-chain peptide bond was formed while the hvdrogen bond to water was broken (FB); the pkptide hydrogen bond was broken and the hydrogen bond to solvent was intact (BF); and 'both hydrogen bonds were simultaneously broken (BB) (Fig. 12). The change in a particular hydrogen bonding arrangement from one structure to the next along the trajectory is given for two temperatures in Table 5. The number of times the conversions occurred is obtained by moving along a row.

At *278* K, when both hydrogen bonds were intact they were likely to remain intact, although there

Table 5

Conversion of the hydrogen bonding arrangements between the peptide and water in a particular structure (N) and in the succeeding structure (N + 1)

N	N+1 FF	FB	BF	BB	BR	TS
A. 278 K						
FF	3645	418	657	16	0	5
FB	412	2517	93	31		
BF	617	85	390	2		
BB	10	32	7	5		
B. 423 K						
FF	395	255	292	33	3	3
FB	218	3013	162	250		
BF	327	136	2846	251		
BB	33	239	261	280		

Average times (ps) for hydrogen bond exchange between peptide and solvent passing through states with both possibilities formed or both. broken

T (K)	FF FB→BF	FF FB→FB	BB FB→BF	BB FB→FB
278	1·0	1·0	0·4	0·4
423	0·5	0·5	0·6	0·4

Moving across a specific row gives the number of times that the hydrogen bonding pattern of N converted to the $N+1$ arrangement. The nomenclature used is given in Fig. 12.

were a large number of cases where one of the two hydrogen bonds broke (FF→FB and FF→BF, Table 5). Once the solvent hydrogen bond was broken (FB), the next structure was most likely to have the same hydrogen bonding pattern, but formation of the water hydrogen bonds was also likely. There were few cases of BF at this temperature (the sum of the entries along the row), and this arrangement usually led to formation of the second hydrogen bond. There were very few situations where both hydrogen bonds were broken or where there was a direct swap of hydrogen bonds (e.g. FB → BF and BF → FB). The average amount of time between FB→BF proceeding through either FF or BB is also given in Table 5, along with the times for reversion to FB. The average times for passing through states with both hydrogen bonds intact was 1·0 picosecond and the conversion was faster for intervening structures with both hydrogen bonds broken, 0·4 picosecond.

The profile was quite different at higher temperature (423 K). There were many fewer cases of formation of both hydrogen bonds. From the FF state, FB and BF were likely. Direct hydrogen bond exchange between FB and BF was more frequent at high temperature although both were most likely to convert, to FF or BB first. Exchange between FB→BF and FB→FB through structures with both hydrogen bonds formed occurred more rapidly at high temperature. The times were comparable for different temperatures for passing through structures with both hydrogen bonds broken, although at 423 K there were many more cases of both hydrogen bonds being broken simultaneously. Hence, at higher temperature. where exchange of the hydrogen bonds was probable, direct concerted exchange did occur but the process was much more likely to pass through intermediate states with both hydrogen bonds intact or both broken.

We then investigated the process of water insertion into the helix. It has been postulated (Sundaralingam & Sekharudu, 1989) that a-helices unfold by formation of a three-centered hydrogen bond between a water molecule and the peptide (TS) from FF. and then the water pries the helix apart, yielding a water molecule bridging the carbonyl and amide groups (BR) (Fig. 12). This process (FF→TS→BR) occurred only once during the simulations, at 423 K. The number of cases of FF → TS was low at all temperatures (Table 5). The number of bridging water molecules increased with increasing temperature (from 0 at 278 K to 221 at 473 K), or unfolding of the helix. There were three cases of direct insertion, FF → BR, which occurred at 423 K. Thus: the bridging water molecules seem to be important as the helix unfolds or in the partially unfolded/unfolded conformations, but unfolding was not caused by the insertion. Rather, the internal helix motion and indirect helix destabilizing effect of the solvent lead to unfolding.

4. Discussion

For many years it was thought that small peptides could not adopt helical conformations in solution. This was due primarly to unsuccessful experimental attempts to detect helical structure in fragments excised from proteins (Epand & Scheraga, 1968) and statistical mechanical models of the helix-coil transition (Schellman, 1958; Peller, 1959*a*,*b*; Schwarz, 1965, 1968; Flory & Miller, 1966; Zimm & Bragg, 1959). Most theoretical treatments of this problem, with the exception of that of Lifson & Roig (1961), assert that propagation should be relatively facile and nucleation difficult, such that long helices are formed rather than short and scattered helical segments. These ideas gained support when the host-guest method was used to experimentally determine the s and σ parameters of the Zimm-Bragg model, where s is the equilibrium constant for helix propagation and σ reflects the likelihood of nucleation. This approach involves introducing an amino acid (guest) into a water soluble homopolymer (host) with a well-characterized helix-coil transition. For L-alanine $s = 1{\cdot}06$ and $\sigma = 8 \times 10^{-4}$ (Scheraga, 1973). These values indicate that the helical state is only favored slightly over the coil state and that nucleation is difficult (e.g. $\sigma = 1$ for no barrier to nucleation). The main physical rationale for this is that propagation of long helices circumvents the entropy cost of bringing residues together to form the first hydrogen bond, as the entropy cost is lower for building onto an existing structure.

In contrast, in our simulations, short helices were highly populated and at times short helical segments were broken by a non-helical segment. A consequence of this behavior is that s and σ are both greater than expected. The intrinsic nucleation parameter, σ, was approximately $0{\cdot}5$, as determined in a previous simulation *in vacuo* (Daggett *et al.*, 1991). It is a bit surprising that the same σ value is obtained *in vacuo* and in solution, as σ would be expected to be lower in solution because of the solvent's ability to stabilize the coil state. Unfortunately, an experimental σ for a small peptide is not available for comparison, but it is usually assumed to be 10^{-3} to 10^{-5}. By fitting our results to the Zimm-Bragg model (as described in Results, section (c), above) the macroscopic σ for our simulations is 10^{-3} to 10^{-4}, in accord with the generally accepted values. The s value from our simulation was dependent on temperature, decreasing with increasing temperature. Near the experimental temperature, 278 K, s was approximately 2. An experimentally derived s value of $1{\cdot}79$ at 273 K for an alanine-based peptide has been reported (Lye *et al.*, 1990). In the previous simulation *in vacuo* an s value of ~ 4 was determined at 400 K (Daggett *et al.*, 1991). This value was thought, to be high because of the lack of solvent. The s value did indeed drop to $\sim$ 1 at this temperature in solution.

From the free energy changes for helix propagation, the enthalpic and entropic contributions to this process were determined. The resulting **AH** for the helix to coil transition ($2{\cdot}1$ kcal/(mol-residue), Results section (c)) is in the vicinity of the results of calorimetric measurements for helix unfolding of an alanine based peptide ($1{\cdot}3$ kcal/(mol-residue); Scholtz *et al.*, 1991) and of polyglutamate ($1{\cdot}1$ kcal/(mol-residue); Rialdi & Hermans, 1966). Although our value is high, the agreement is gratifying given that, our definition of helix content has not been calibrated against experiment. The values for propagation of the helix were used in lieu of those for the single residue transitions because Scholtz et *al.* (1991) have suggested that circular dichroism and calorimetric probes monitor the same unfolding events. There must be some critical number of helical residues to give a circular dichroism signal (Manning *et at.*, 1988) and single isolated, helical residues within a peptide should not contribute much to the signal.

In the earlier simulation of polyalanine *in vacuo* the transition rate for a single residue propagating a helix was 10^{10}/s (Daggett *et al.*, **1991).** The experimental results suggest rate constants of 10^{7} to 10^{10}/s for a variety of polypeptides in different solvents (Bosterling & Engel, **1979;** Gruenewald *et al.*, 1979; Inoue *et al.*, **1979;** Tsuji *et al.*, **1976).** It was thought that the value determined from the simulation was at the high end of the experimental range because of the use of high temperature (400 K) and the lack of solvent (the value will also depend on the definition of h and c, of course). These two possibilities can now be ruled out. The simulations in solution presented here also yield an approximate transition rate of 10^{10}/s **(3** to 9 transitions/100 ps) for all of the temperatures investigated. Therefore, the value is still at the high end of the experimental range but is reasonable. Also, the time scale of the structural changes that take place during the simulations appears to be reasonable, as the diffusion of the water molecules as a function of temperature is similar to the experimental values: $0{\cdot}13$ to $1{\cdot}80$ Å^2/ps between 278 and 473 K in the simulation *versus* $0{\cdot}14$ to $2{\cdot}87$ Å^2/ps experimentally for pure water (the experimental values below 323 K were taken from Table 4.7 of Eisenberg & Kauzmann (1969), the values at higher temperatures were estimated from the viscosity data in Table 4.8); however, water diffusion decreases in biopolymer solutions (Cook & Kuntz, **1974).** Diffusion is one of the few time-dependent properties that can be determined directly both experimentally and from the simulations.

Experimentally, small helices are marginally stable in solution and unlike longer polypeptides do not show co-operative melting curves. In the simulations presented here the peptide was stable as an a-helix at low temperature and melted with increasing temperature. This is consistent with the experimental studies, although in the simulations the peptide was too stable at moderate-high temperatures with denaturation spanning $\sim 120^{\circ}$. For comparison, unfolding of a polyalanine- based peptide spans $\sim 70^\circ$ experimentally (Marqusee *et al.*. 1989). However. our simulations were short, and, given the drop in helix content with time (Fig. 4). the unfolding range would presumably decrease in longer simulations. With increasing temperature the coil state became more favorable than the helical state and the free energy of activation of the $c \rightarrow h$ transition increased with temperature. making it difficult for a non-helical residue to return to the helical state. The behavior of the free energy of activation was due predominantly to the entropic difficulty in adopting the transition state structure from progressively more disordered non-helical conformations.

Most unfolding steps involved the loss of local helical structure. 'At low temperature. these transitions led to fluctuations about the helical conformation. A successive loss of local structure resulted in more global unfolding. The more global unfolding steps began as fraying at the ends of the helical segments or unfolding 'within the helix. The latter tye of unfolding usually involved a kink in the structure. which was then propagated. Tn some cases these kinks or turns were stabilized through hvdrogen bonds with water and non-ideal (other than $i \rightarrow i+4$) intrachain hydrogen bonds were formed. But. this mechanism of unfolding is not dependent on the presence of water molecules, as the same behavior was observed *in vacuo* both here and in a previous simulation (Daggett *et al.*. 1991). Formations of these kinks or turns often facilitated further unfolding. In the case of refolding. helix formation was often initiated at turns.

Tn our simulations. the peptide spent the bulk of its time fluctuating between conformations with intermediate helix content at all but the highest temperature. Fractions of helix are observed in small peptides using circular dichroism. Furthermore. specific regions of helix along the sequence have been identified using two-dimensional nuclear magnetic resonance experiments (Bradley *et al.*. 1990: Fry *et al.*. 1989: Lyu *et al.*. 1990: Osterhout et *al.*. 1989). Thus. small' peptides appear to be made up mostly of structures with intermediate helix contents. as opposed to an equilibrium between 0% and 100% helical structures. In the simulations. the peptide was stable even with short helical segments broken by a non-helical region. Conservation to highly helical conformations proceeded from these short 'helical fragments and both nucleation and propagation were relatively facile. Tn the case of a protein, just the formation of this type of transient structure may aid folding by limiting the conformational space that needs to be sampled and allowing a framework onto which further structural elements can dock or allowing on-site folding to occur. The different conformations of the peptide interconverted readily. implying that different conformations could be searched quickly during protein folding while preventing the ''freezing' of incorrect conformations.

The presence of water facilitated $h \rightarrow c$ transitions. or unfolding. while inhibiting $c \rightarrow h$ conversions. or refolding. Thus, water acted as a denaturant and, in fact, small peptides show increased helicitp in trifluoroethanol. for example. compared to water (Nelson & Kallenbach. 1986). However. the effect of water on the peptide was relatively non-specific. The polar peptide atoms had more of an effect on the orientations of the surrounding water molecules than did the non-polar groups, but this effect diminished with increasing temperature. At low temperature most of the water molecules in contact with the polar atoms formed hydrogen bonds. In fact, most of the peptide carbonyl groups in the structures at low temperature formed both intrapeptide and water hydrogen bonds simultaneously. At high temperature (but below 473 K) and decreased water density. the peptide became partially unfolded, the number of main chain-water contacts increased slightly but the number of hydrogen bonds decreased. At 473 K. however? both 'the number of water-main chain contacts and hydrogen bonds increased as expected with increases in the accessible surface area. Therefore. the exposure of the backbone in the completely unfolded state ordered the nearby water molecules. To achieve this effect the peptide had to overcome both the decrease in density (and therefore lower probability of having water molecules nearby) and the increased water disorder.

Most of the occurrences of hydrogen bond exchange from FB (having the intrapeptide hydrogen bond formed and the 'hydrogen bond to water broken) to BF (a broken intrapeptide hydrogen bond and intact hydrogen bond with' water) proceeded through intermediate structures with either both of the hydrogen bonds formed or both broken. in lieu of concerted direct exchange. Sundaralingam & Sekharudu (1989) surveyed crystal structures with hydrated α-helices and found a number of cases of inserted water molecules. On the basis of this observation. they postulated that carbonyl groups are hydrated in the helical conformation (FF). then a three-centered hydrogen bond is formed (TS). The water molecule then inserts itself between the carbonyl and amide groups. acting as a bridge (RR). which will favor formation of turns. They propose that this process describes the folding/unfolding pathway of a-helices. We did not find this to be an important mode of unfolding in our simulations. In fact, it was observed only once in all of the simulations. We did, however, find numerous bridging waters, the occurrence of which increased with temperature, which is consistent with Sundaralingam & Sekharudu's contention that bridging water molecules are associated with destabilization of the helix. This effect has also been observed in another simulation by DiCapua *et al.* (1990). The Ramachandran maps generated during the simulations show movement away from the α-helix region of conformational space towards the P-region with increasing temperature. Sundaralingam & Sekharudu (1989) also observed these intermediate conformations in what they call the elbow region of the map. Thus, our findings do indeed suggest that bridging water molecules are important during unfolding and correlate with turn formation. However. contrarv to Sundaralingam & Sekharudu's proposal, the bridging water molecule is not arrived at directly by concerted attack. Instead the process is due to the inherent motion of the helix and the non-specific denaturing effect of water.

The solvent did. however, interact strongly and favorably with the peptide in its partially unfolded form but not predominantlv through specific hydrogen bonds. Therefore, the intramolecular hydrogen bonds of the helical state were not fullv compensated by hydrogen bonds to solvent in the partially unfolded forms of the peptide. These partially unfolded forms are presumably the types of structures present experimentally; but because of the increased mobility and transient nature of the intramolecular hydrogen bonds at higher temperatures, the atoms were not aligned properly on average for formation of hydrogen bonds. The lower water density at high temperature also contributes to the decreased peptide-water interactions. Therefore. increases in temperature not only disrupted the structure of the peptide but also the peptide-water interactions.

We thank I. D. Kuntz for helpful discussions and suggestions when this work was going on. as well as for useful comments on the manuscript. This work was supported by the NIH (GM-41455 to M.L.) and aided by a grant from the Jane Coffin Childs Memorial Fund for Medical Research (to V.D.).

References

Bierzynski, A.. Kim. P. S. & Baldwin. R. L. (1982). A salt bridge stabilizes the helix formed by isolated C-peptide of RNase A. *Proc. Nat. Acad. Sci.. U.S.A.* 79. 2470–2474.

Bosterling. B. & Engel. J. (1979). Kinetic studies on the helix-coil transition of fluorescent labeled poly-(L-lysine) by the temperature-jump technique. *Biophys. Chem.* 9. 201–209.

Bradley. E. K.. Thomason. J. F.. Cohen. F. E.. Kosen. P. A. & Kuntz. I. D. (1990). Studies of synthetic helical peptides using circular dichroism and nuclear magnetic resonance. *J. Mol. Biol.* **215.** 607–622.

Brown, J. E. & Klee. W. A. (1971). Helix-coil transition of the isolated amino terminus of ribonuclease. *Biochemistry*, **10.** 470-476.

Cooke. R. & Kuntz. I. D. (1974). The properties of water in biological systems. *Annu. Rev. Biophys. Bioeng.* 3. 95-126.

Daggett. V.. Kollman. P. A. & Kuntz. I. D. (1991). A molecular dynamics simulation of polyalanine: an analysis of equilibrium motion and helix-coil transitions. *Biopolymers*, 3 **1.** 1115–1134.

DiCapua. F. M.. Swaninathan. S. & Beveridge. D. L. (1990). Theoretical evidence for destabilization of an c-helix by water insertion: molecular dynamics of hydrated decaaline. *J. Amer. Chem. Soc.* **112.** 6768–6771.

Eisenberg. D. & Kauzmann. W. (1969). *Structure and Properties of Water,* Clarendon Press. Oxford.

Epand. R. M. & Scheraga. H. A. (1968). The influence of long-range interactions on the structure of myoglobin. *Biochemistry, 7,* 2864-2872.

Fieser. T. M.. Tainer. J. A., Gevsen. H. M.. Houphten. R. A. & Lerner. R. A. (1987). Influence of protein flexibility and peptide conformation on reactivity of monoclonal anti-peptide antibodies with a protein α-helix. *Proc. Nat. Acad. Sci.. U.S.A. 84.* 8568–8572.

Flora. P. J. & Miller. W. G. (1966). A general treatment of helix-coil equilibria in macromolecular systems. *J. Mol. Biol.* **15. 284-297.**

Fry D. C.. Madison. V. S.. Bolin. D. R.. Greeley. D. N.. Toome. V. & Wegrzynski. B. B. (1989). 'Solution structure of an analogue of vasoactive intestinal peptide as determined by two-dimensional NMR and circular dichroism spectroscopies and constrained molecular dynamics. *Biochemistry. 28.* 2399–2409.

Goodman. E. M. & Kim. P. S. (1989). Folding of a peptide corresponding to the g-helix in bovine pancreatic& trypsin inhibitor. *Biochemistry. 28.* 4343–4347.

Gruenewald. B.. Sicola. C. U.. Lustig. A.. Schwarz. G. & Klump. H. (1979). Kinetics of the helix-coil transition of a polypeptide with non-ionic side groups. derived from ultrasonic relaxation measurements. *Biophys. Chem. 9,* 137-147.

Inoue. S., Sano. T.. Yakabe. Y.. Ushio. H. & Yasunaga. T. (1979). Kinetic studies of the helix-coil transition in aqueous solutions of poly(L-lysine). *Biopolymers,* **18.** 681-691.

Kabsch. W. (1976). A solution for the best rotation to relate two sets of vectors. *Acta Crystallogr. sect A. 32. 922-923.*

Kell. G. S. (1967). *J. Chem.* Eng. *Data.* 12. 66.

Kim. P. S. & Baldwin. R. L. (1982). specific intermediates in the folding reactions of small proteins and the mechanism of protein folding. *Annu. Rev. Biochem.* **51. 459-489.**

Lee. B. & Richards. F. M. (1971). The interpretation of protein structures: estimation of static accessibility. *J. Mol. Biol.* 55. 379–400.

Levitt. M. (1983). Molecular dynamics of native proteins. I. Computer simulation of trajectories. *J. Mol. Biol.* **168. 595-620.**

Levitt. M. (1989). Molecular dynamics of macromolecules in water. *Chem. Scripta.* **29A.** 197–203.

Levitt. M. (1990). *ENCAD Energy Calculations and Dynamics.* Stanford University.

Levitt. M. & Sharon. R. (1988). &curate simulation of protein dynamics in solution. *Prof. Sat. Acad. Sci.. U.S.A.* 85. 75X-7561.

Lifson. S. & Roig. A. (1961). On the theory of helix-coil transition in polypeptides. *J. Chem. Phys. 34.* 1963-1974.

Lyu. P. C.. Liff. M. I.. Marky. L. A. & Kallenbach. N. R. (1990). Side-chain contributions to the stability of x-helical structure in peptides. Science. 250. 669–673.

Manning. M. C.. Illangasekare. M. & Woody. R. W. (1988). Circular dichroism studies of distorted α-sheets. and p-turns. *Biophys. Chem.* **31.** 77–86.

Marqusee. S. & Baldwin. R. L. (1987). Helix stabilization by Glu$^-$... Lys$^+$ salt bridges in short peptides of de novo design. *Proc. Nat. Acad. Sci.. U.S.A. 84.* 8898–8902.

Marqusee. S.. Robbins. V. H. & Baldwin. R. L. (1989). Unusually stable helix formation in short alanine-based peptides. *Proc. Nat. Acad. Sci., U.S.A. 86. 52864290.*

Nelson, J. W. & Kallenbach, IS. R. (1986). Stabilization of the ribonuclease S-peptide a-helix by trifluoroethanol. *Proteins,* **1. 21 l-217.**

Osterhout, J. J.. Jr. Baldwin. R. L.. York, E. J ., Stewart. J. M.. Dyson, H. J. & Wright. P. E. (1989). [1]H NMR studies of the solution conformations of an analogue of the c-peptide of ribonuclease A. *Biochemistry, 28, 7059-7064.*

Peller, L. **(1959a).** On a model for the helix-random coil transition in polypeptides. I. The model and its thermal behavior. *J. Phys. Chem.* **63,** 1194-1199.

Peller, L. **(1959b).** On a model for the helix-random coil transition in polypeptides. II. The influence of solvent composition and charge interactions on the transition. *J. Phys. Chem. 63.* **1199-1206.**

Ptitsyn, 0. B. & Rashin, A. A. **(1975).** A model of myoglobin self-organization. *Biophys. Chem. 3,* 1-20.

Rialdi, G. & Hermans, J., Jr. **(1966).** Calorimetric heat of the helix-coil transition of poly-L-glutamic acid. *J. Amer. Chem. Soc. 88,* 5719-5720.

Schellman, J. **A. (1958).** The factors affecting the stability of hydrogen-bonded polypeptide structures in solution. *J. Phys. Chem. 62,* **1485-1494.**

Scheraga. H. (1973). On the dominance of short-range interactions in polypeptides and proteins. *Pure and Appl. Chem. 36.* **l-8.**

Scholtz, J. M., Marqusee, S., Baldwin, R. L.. York, E. J., Steward. J. M., Santoro. M. & Bolen. D. W. **(1991).** Calorimetric determination of the enthalpy change for the c-helix to coil transition of an alanine peptide in water. *Proc. Nat. Acad. Sci., U.S.A. 88, 2854-*2858.

Schwarz, G. (1965). On the kinetics of the helix-coil transition of polypeptides in solution. *J. Mol. Biol.* **11, 64-77.**

Schwarz, G. **(1968).** General theoretical approach to the thermodynamic and kinetic properties of cooperative intramolecular transformations of linear biopolymers. *Biopolymers, 6. 873-897.*

Shoemaker, K. R., Kim, P. S., Brems, D. N., Marqusee, S., York, E. J., Chaiken, I. M., Stewart, J. M. & Baldwin. R. L. **(1985).** Nature of the charged-group effect' on the stability of the C-peptide helix. *Proc. Nat. Acad. Sci., U.S. A. 82, 2349-2353.*

Shoemaker. K. R., Kim, P. S., York, E. J., Stewart, J. M. & Baldwin, R. L. (198'7). Tests of the helix dipole model for stabilization of α-helices. *Nature (London),* **326,** 563-567.

Sundaralingam. M. & Sekharudu. Y. C. **(1989).** Water-inserted c-helical segments implicate reverse turns as folding intermediates. *Science, 244,* **1333-1337.**

Tainer, J. A., Getzoff, E. D., Alexander, H., Houghten, R. A., Olsen, A. J., Lerner, R. A. & Hendrickson, W. A. **(1984).** The reactivity of anti-peptide antibodies is a function of the atomic mobility of sites in protein. *Nature (London), 312, 127-134.*

Takahashi. S. **(1990).** Conformation of membrane fusion-active 20-residue peptides with or without lipid bilavers: implication of a-helix formation for membrane fusion. *Biochemistry, 29. 6257-6264.*

Tsuji. Y., Yasunaga. T., Sano, T. & Ushio, H. (1976). Kinetic studies of the helix-coil transition in aqueous solutions of poly(α-L-glutamic acid) using the electric field pulse method. *J. Amer. Chem. Soc. 98,* **813-818.**

Vogel, H., Nilsson, L., Rigler, R., Voges, K. & Jung, G. **(1988).** Structural fluctuations of a helical polypeptide traversing a lipid bilayer. *Proc. Nat. Acad. Sci., U.S.A. 85, 5067-5071.*

Zana, R. **(1975).** On the rate-determining step for helix propagation in the helix-coil transition of polypeptides in solution. *Biopolymers,* **14, 2425-2428.**

Zimm, B. H. & Bragg, J. K. **(1959).** Theory of the phase transition between helix and random coil in polypeptide chains. *J. Chem. Phys.* **31, 526-535.**

Edited by P. von Hippel